J Mol Model (2012) 18:2993–3001
DOI 10.1007/s00894-011-1314-y

ORIGINAL PAPER

Structural, electronic and magnetic effects of Al-doped niobium clusters: a density functional theory study

Huai-Qian Wang · Hui-Fang Li · Jia-Xian Wang · Xiao-Yu Kuang

Received: 12 July 2011 / Accepted: 16 November 2011 / Published online: 7 December 2011

Abstract The application of the ab initio stochastic search procedure with Saunders "kick" method has been carried out for the elucidation of global minimum structures of a series of Al-doped clusters, Nb_nAl ($1 \le n \le 10$). We have studied the structural characters, growth behaviors, electronic and magnetic properties of Nb_nAl by the density functional theory calculations. Unlike the previous literature reported on Al-doped systems where ground state structures undergo a structural transition from the Al-capped frame to Al-encapsulated structure, we found that Al atom always occupies the surface of Nb_nAl clusters and structural transition does not take place until $n=10$. Note that the fragmentation proceeds preferably by the ejection of an aluminum atom other than niobium atom. According to the natural population analysis, charges always transfer from aluminum to niobium atoms. Furthermore, the magnetic moments of the Nb_nAl clusters are mainly located on the 4d orbital of niobium atoms, and aluminum atom possesses very small magnetic moments.

Keywords Density functional theory · Electronic properties · Magnetic properties · Nb_nAl clusters

Introduction

Niobium clusters have received considerable attention from a wide range of researchers in recent years [1–28]. On the experimental side [1–14], earlier experiments mainly dealt with the mass, optical, photoelectron, and infrared spectrometries of small Nb clusters. Nb clusters of various sizes have been produced by pulsed laser vaporization of compressed Nb powder [8, 9]. A series of experiments on the reactiviey of Nb clusters have also been performed using fast flow reactor techniques [10–12], flow tube [13], and guided ion beam measurements [14], and the results show interesting size effects in their gas phase reactivity, e.g., toward hydrogen, nitrogen, or small hydrocarbons and so on. On the theoretical side [15–28], theoretical studies on Nb clusters show they have low symmetry in comparison with other clusters such as Ti_n,Y_n and Sc_n. The ground states of Nb clusters always tried to remain in their lowest possible spin state, expect for Nb_2. However, for the small Nb clusters, the optimal geometries and ground state symmetry of Nb clusters are sensitive to the choice of functionals and basis sets. Majumdar and Balasubramanian [16] reported the ground state of Nb_3 is $^2B_1(C_{2v})$ state at B3LYP and MRSDCI level. This agreed with the results of Fowler and coworker [20], but disagreed with DFT results of Goodwin et al. [19] and Kumar et al. [15] who reported a $^2A_2$ ground state for Nb_3. Zhai and coworker [21] predicted the distorted $^2A''$ (C_s) triangular structure for the ground state of Nb_3. Nhat and coworker [22] studied a series of small Nb_n ($n=2$–6) and their cations and anions using CCSD(T), B3LYP, BLYP, BP86, and BPW91 functionals and obtained that BLYP, BP86 and BPW91 functionals predicted a $^2A_2$ ground state for the C_{2v} isosceles trigangle Nb_3 while B3LYP function predicts a $^2B_1$ ground state. Since the ground states structures of Nb clusters depend on the theoretical method, in the present calculation, three different density functional theory methods are used for the studied systems to ensure the accuracy of calculation. Apart from the fundamental understanding of the geometries of Nb clusters, many theoretical studies on Nb clusters have focused on the reactivities of Nb clusters with H_2, D_2, N_2, and

H.-Q. Wang (✉) · H.-F. Li · J.-X. Wang
College of Engineering, Huaqiao University,
Quanzhou 362021, China
e-mail: hqwang@hqu.edu.cn

H.-F. Li · X.-Y. Kuang
Institute of Atomic and Molecular Physics, Sichuan University,
Chengdu 610065, China

CO [23–26]. Reactivities of niobium clusters with hydrogen show dramatic size dependence that is quite different from the behavior known for clusters of some other transition metal such as nickel. Similar studies [26] of CO reactivity with Ni and Nb clusters also show different behaviors with a distinct minimum for Nb_{10}. Photoemission studies on niobium clusters suggest large HOMO-LUMO gaps for 8-, 10-, and 16-atom clusters, corresponding to the low reactivities.

Doped clusters are important as they can provide new physicochemical properties that are different from those in the pure clusters. Among the doped clusters, the Al atom as an impurity atom has attracted the attention of many researchers [29–36]. Xiang and coworkers [29] studied the equilibrium geometries, stabilities, and electronic properties of Ti_nAl (n=1–13) using density functional theory, and they concluded that the structural transition takes place at n=9. Al atom remains on the surface of clusters for n<9, but is slowly getting trapped beyond n=9. Similar to growth pattern of Ti_nAl (n=1–13), recent theoretical studies by Zhao et al., [30] Wang et al. [34] and Tian et al. [35] also predicted positional change of impurity Al atom in Y_nAl,Sc_nAl and Pb_nAl clusters at n=9. Theoretical study on geometries and electronic properties of Si_nAl [31] has shown that Si_nAl (n= 1–11) is obtained by replacing one of the Si atoms of Si_{n+1} cluster. However, the study of B_n and B_nAl clusters [32] found that the lowest-energy structures of B_nAl can be obtained by adding one Al atom on the stable B_n. Although several reports are available on the interaction of the Al atom as an impurity with metal clusters, the studies on Al-doped niobium cluster are very few to our knowledge. Pure Nb cluster displays different properties from other transition metals on reactivity with H_2 and D_2, and it is wondered whether the Al-doped Nb clusters have some different behaviors from the other similar Al-doped clusters? It would be interesting and valuable to compare their geometries, stabilities, and electronic properties with similar M_nA1 clusters.

In this work, we present theoretical investigation of a series of Al-doped clusters, Nb_nAl ($1 \le n \le 10$). The main objectives of this paper are (1) to obtain the various global minimum structures of Nb_nAl by means of three functionals, (2) to study the growth behaviors, electronic and magnetic properties of Al-doped clusters. This work should be interesting for future theoretical and experimental chemists, especially those designing new materials.

Computational methods

The ground states of the Nb_nAl ($1 \le n \le 10$) clusters were determined by means of generalized gradient approximation to DFT using GAUSSIAN 03 programs [37]. We first performed the search for the global minima on the potential energy surface (PES) for Nb_nAl ($1 \le n \le 10$) systems using the Saunders "kick" method [38–40]. This stochastic method generates structures randomly and facilitates the thorough exploration of unknown isomers much more easily than manual methods. In order to avoid biasing the search, all the atoms are placed at the same point initially and then are "kicked" randomly within a sphere of radius R (R is the maximum kick distance). The kick method runs at the B3PW91/3–21G level some 500 times ($n \ge 6$) until no new minima appeared. Afterward, the isomers were ranked according to their relative energies at the B3PW91/3–21G level. Next, the top ranked 10–30 isomers were further optimized and refined with the larger basis set. In order to ensure the accuracy of calculation and gain insight into the performance of different methods, three different DFT methods were used. The first DFT method is the B3PW91 method [41–44], which uses Perdew-Wang 91 for correlation and Becke-3 for exchange functional method. The second method is the B3LYP method [41, 45], which uses Becke's three-parameter functional with the Lee-Yang-Parr correlation functional. The third DFT method is Perdew-Burke-Ernzerhof exchange and correlation functional (PBEPBE) [46]. The triple-ζbasis sets, 6-311G(d), were used for Al atom, and the LANL2DZ basis set, which involves the Los Alamos effective core potential plus a double zeta basis set, is employed to model the Nb atom. Vibrational frequency calculations were performed at the corresponding level of theory to verify the nature of the stationary points. The results obtained by three functionals are essentially identical, this is consistent with previous tests for the accuracy and consistency of several exchange-correlation functionals [47, 48]. Since no symmetry constraints are imposed, the geometries obtained should correspond to the global minimum structures. Different possible spin multiplicities were also considered for each of these structural isomers to determine the preferred spin states of these complexes. Spin-restricted DFT calculations were employed for the singlet state, while spin-unrestricted DFT calculations were employed for all other electronic states.

Results and discussion

Geometries of Nb_nAl ($1 \le n \le 10$)

The ground state geometries of Nb_nAl ($1 \le n \le 10$) clusters and some low-lying isomers are shown in Fig. 1 and Table 1. According to the total energy from low to high, the low-lying isomers are designated by Na, Nb and Nc for the Nb_nAl clusters and Na_0 represents the pure Nb_n clusters. ("N" is the number of Nb atoms.) In order to compare the structure difference between the pure Nb_n and doped Nb_nAl clusters and discuss the effects of doped impurity atom on Nb_n clusters, we have also shown the ground state geometries of

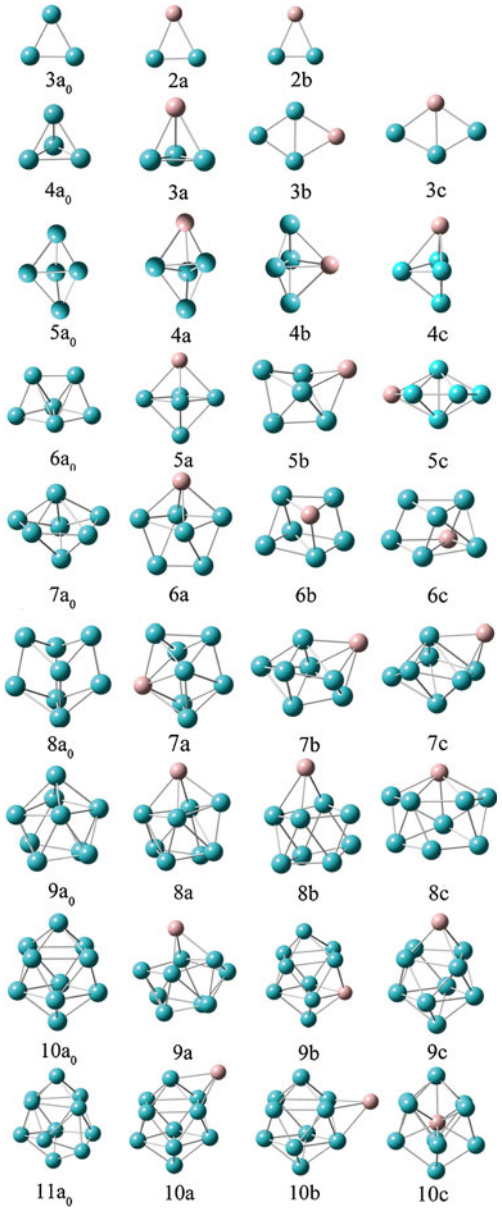

Fig. 1 Lowest-energy structure of $Nb_n(2\leq n\leq 11)$ clusters and lowest-energy and low-lying structures of $Nb_nAl(1\leq n\leq 10)$ clusters

$Nb_n(2\leq n\leq 11)$ clusters. It must be pointed out that for pure Nb_n clusters only B3PW91 method in conjunction with the LANL2DZ basis set is used for the geometry optimization and vibrational frequency calculation. We will compare the results of Nb_nAl with pure Nb_n clusters and also compare them with the results for Ti_nAl [29], Y_nAl [30], Si_nAl [31], B_nAl [32], Na_nAl [33], Sc_nAl [34], and Li_nAl [35] clusters.

For the NbAl cluster, the lowest-energy structure is a septet state with $C_{\infty v}$ symmetry by three functionals. The similar quintet isomer lies energetically above septet by 0.651 eV (B3PW91), 0.425 eV (B3LYP), 0.617 eV (PBEPBE), respectively. Nb_3 clusters have been extensively investigated in previous studies and a substantial debate has been already generated on the electronic state as mentioned in the first section. The electronic state and point symmetry of Nb_3 are sensitive to the choice of method. For Nb_3, DFT computation predicts isomer $3a_0$ (C_s symmetry) as the global minimum structure. For Nb_2Al, the lowest-energy structure is either a doublet C_s structure (2a in Fig. 1) or a quartet C_{2v} structure (2b in Fig. 1), depending on the theoretical method. The B3PW91 method predicts 2a to lie lower in energy than 2b by 0.109 eV, while the B3LYP and PBEPBE methods predict 2a to lie higher than 2b by 0.095 eV and 0.028 eV, respectively. Thus structure 2a and 2b are essentially degenerate in energy. Nb_3Al is the first three-dimensional (3D) structure which can be obtained by substituting one Al atom for one Nb atom located at one apex of

Table 1 Spin multiplicities (M), point group symmetry (PGS) and relative energies respect to the lowest-energy structure (ΔE) by B3PW91, B3LYP, and PBEPBE functionals

System	Isomer	M	PGS	ΔE(eV)		
				B3PW91	B3LYP	PBEPBE
NbAl	1a	7	$C_{\infty v}$	0	0	0
		5	$C_{\infty v}$	0.651	0.425	0.617
Nb_2Al	2a	2	C_S	0	0.095	0.028
	2b	4	C_{2v}	0.109	0	0
Nb_3Al	3a	3	C_s	0	0	0
	3b	1	C_{2v}	0.273	0.094	0.081
	3c	5	C_{2v}	1.288	1.232	0.295[a]
Nb_4Al	4a	2	C_s	0	0	0
	4b	2	C_{2v}	0.269	0.331	0.298
	4c	2	C_s	0.482	0.447	0.527
Nb_5Al	5a	1	C_{2v}	0	0	0
	5b	1	C_1	0.516	0.441	0.508
	5c	1	C_s	0.650	0.586	0.617
	5d	1	C_1	1.138	1.071	1.127
Nb_6Al	6a	2	C_1	0	0	0
	6b	2	C_1	0.677	0.602	0.591
	6c	2	C_1	1.008	0.918	0.988
Nb_7Al	7a	1	C_1	0	0	0
	7b	1	C_1	0.399	0.371	0.436
	7c	1	C_s	0.457	0.416	0.430
Nb_8Al	8a	2	C_1	0	0	0.017
	8b	2	C_1	0.039	0.002	0
	8c	2	C_1	0.420	0.432	0.390
Nb_9Al	9a	1	C_1	0	0	0
	9b	1	C_1	0.070	0.051	0.155
	9c	1	C_1	0.345	0.295	0.369
$Nb_{10}Al$	10a	2	C_s	0	0	0
	10b	2	C_1	0.130	0.122	0.189
	10c	2	C_1	1.353	1.751	1.571

[a] Spin multiplicities is $M=1$

pyramid of the Nb_4 frame. The geometries of Nb_3Al is a little distortion compared to that of Nb_4. The point group symmetry of Nb_3Al structure with the triplet state is C_s symmetry. For the similar Al-doped clusters, Nb_3Al has relatively low symmetry compared to other clusters such as $Ti_3Al(C_{3v})$ [29], $Y_3Al(C_{3v})$ [30], $B_3Al(C_{2v})$ [32], Sc_3Al (C_{3v}) [34]. Here, it should be mentioned that most of the Nb_nAl clusters have relatively low symmetry in comparison with other Al-doped clusters, this can be seen in the following discussion on geometry structures of the Nb_nAl clusters. Structures 3b and 3c are both the planar rhombus with C_{2v} symmetry and the difference between the two isomers is the position of the impurity atom Al. Our calculation determined that the structures 3b and 3c are higher in energy than the lowest-energy structure 3a by 0.273 eV and 1.288 eV (B3PW91), 0.094 eV and 1.232 eV (B3LYP), 0.081 eV and 0.295 eV (PBEPBE), respectively. For the isomer 3c, the energy order of different spin states obtained by the three functionals is somewhat different. B3PW91 and B3LYP methods predict the lowest-energy 3c structure is a high spin quintet state, while PBEPBE method predicts singlet state corresponds to a lower energy. However, the ground state structure obtained by three functionals is consistent. The lowest-energy structure of Nb_4Al with a doublet state is a distorted trigonal bipyramid. Nb_4Al can be obtained by substituting one Al atom for one Nb atom located at one apex of bipyramid of the Nb_5 frame. It can also be created by adding one Nb atom on the peripheral site of the stable Nb_3Al. Again note the symmetry of Nb_4Al cluster. Nb_4Al is C_s symmetry similar to Nb_5 cluster, while for most of the mixed Al-doped clusters, for example, Ti_4Al, Y_4Al, Sc_4Al, a triangle bipyramid structure with C_{3v} symmetry has been proven to be most stable. The same symmetry C_s is only found for B_4Al cluster. Another structure 4b with Al atom sitting on the trigonal ring of the bipyramid is 0.269 eV (B3PW91), 0.331 eV (B3LYP), 0.298 eV (PBEPBE) higher than ground state structure 4a. Structure 4c, which is similar to structure 4a, is higher in energy than isomer 4a by 0.482 (B3PW91), 0.447(B3LYP) and 0.527 eV (PBEPBE), respectively. Nb_5Al is the first cluster whose geometry differs significantly from a pure Nb_6 cluster. Nb_6 is a dimer-capped rhombus, which is consistent with the results of Goodwin et al. [19]. and Nhat et al. [22]. However, Nb_5Al form an octahedron configuration with Al atom at the vertex. It can be generated by capping one Nb atom to the most stable structures of Nb_4Al. The lowest-energy structure of Nb_5Al is a spin singlet, more stable in energy than the triplet state by 0.111 eV (B3PW91), 0.441 eV (B3LYP), 0.508 eV (PBEPBE). The dimer-capped rhombus 5b is higher than 5a by 0.516 eV (B3PW91), 0.441 eV (B3LYP), 0.508 eV (PBEPBE). Structure 5c can be viewed as a bipyramid structure, which is 0.650 eV by B3PW91, 0.586 eV by B3LYP, and 0.617 eV by PBEPBE higher than structure 5a. Nb_7 is a distorted pentagonal bipyramid as also obtained earlier in Ref 15. From the point of view of growth, it is interesting that the doped Nb_6Al cluster can be viewed as the one obtained from capping of an Al atom to the Nb_6 structure, or from replacing one Nb atom by Al atom occupying one corner of the base pentagon of Nb_7 structure. The ground state geometry of Nb_6Al is C_1 symmetry with the pentagonal Nb_5 a little distorted in comparison with pure Nb_7 structure. The similar shape is found but with higher symmetry for $Ti_6Al(D_{5h})$ [29], Y_6Al (C_{2v}) [30], $Sc_6Al(C_{2v})$ [34]. For Al-doped B cluster, the same pentagonal bipyramid structure with C_1 point symmetry is found for B_6Al, however, for Na_6Al and Li_6Al, the structural transition from the Al-capped structure to the Al-encapsulated structure appears at n=6. The Al atom gets trapped inside the Na and Li cages and is almost at the center of mass of the clusters. We also consider the Al-encapsulated structure as the initial structure, but the Al atom moves from the center to the surface of the cluster during the geometry optimization process. It is clear from Fig. 1 that capping of an Al atom or Nb atom to the Nb_6 structure but with a different position produces several different structures 6b, 6c. Structures 6b and 6c lie above the lowest-energy structure 6a by 0.677, 1.008 eV (B3PW91), 0.602, 0.918 eV (B3LYP), 0.591, 0.988 eV (PBEPBE). For Nb_7Al, we tried several structures such as capped prism and a capped octahedron. The lowest-energy structure is a bicapped distorted octahedron and can be created by taking the most stable isomer of Nb_8 and substituting one Nb atom for Al atom. An Al atom capped on the distorted pentagonal bipyramid of Nb_7 yields the low-lying structures 7b and 7c. They are about 0.399, 0.457 eV (B3PW91), 0.371, 0.416 eV (B3LYP), 0.436, 0.430 eV (PBEPBE) less stable relative to structure 7a. Here, PBEPBE method predicts the 7c has slightly lower energy than 7b, this order is inconsistent with the results obtained by B3PW91 and B3LYP methods. Structures 8a and 8b of Nb_8Al is also a substitutional structure with the Al atom replacing the top Nb atom with small local distortion. The shape of both isomers closely resembles each other. Isomer 8a is predicted to be the lowest-energy structure by B3PW91 and B3LYP methods, while it is predicted by the PBEPBE method to lie above structure 8a by 0.017 eV. The small relative energies and similar structure of 8a and 8b suggest the two isomers are degenerate. Another 8c lies higher than 8a by 0.432 eV (B3PW91), 0.338 eV (B3LYP), 0.322 eV (PBEPBE).

Several Al-doped clusters, such as Ti_nAl [29], Y_nAl [30], Sc_nAl [34], Pb_nAl [35], undergo a structural transition from the Al-capped frame to Al-encapsulated structure at n=9, while the structural transition appears prematurely at n=6 for Na_nAl and Li_nAl, and B_nAl and Si_nAl do not experience the structure transition until n=12 and n=10, respectively. This is mainly due to the different ionic radii of Al and host

atoms and different bond strength of Al-M and M-M bonds. However, what will happen for Nb_nAl cluster? Is the Al atom adsorbed on the surface or located in the center of the Nb_n frame? Several initial geometries including the Al-encapsulated structures were considered to obtain the lowest-energy structure of the Nb_9Al cluster. Our calculation shows after geometry optimization the Al atom Al atom can not be encapsulated inside the Nb_{10} cluster and still remain on the surface of the lowest-energy Nb_9Al cluster using three methods and the structural transition does not occur until n=9. Structure 9a is the capped structure where the Nb atom is capping one of the triangular faces of the lowest-energy structure 8a. Another substitutional structures 9b and 9c with the substitution for Nb_{10} but with a different substituting position of Nb atom are higher in energy, 0.070 and 0.345 eV by B3PW91, 0.051, and 0.295 eV by B3LYP, 0.155 and 0.369 eV by PBEPBE, than lowest-energy structure 9a.

We have also considered the initial geometry with Al-encapsulated and Al-capped structures. For the $Nb_{10}Al$ cluster, the lowest-energy structure was found to be a capped bicapped antiprism where the Al atom is capping one of the triangular faces of the Nb_{10} structure. When the doped Al atom is added to the stable structure of Nb_{10} at different position from structure 10a, a new structure 10b is formed, but 0.130 eV by B3PW91, 0.122 eV by B3LYP, 0.189 eV by PBEPBE higher than 10a. The Al-encapsulated structure is found in the present study but at high energy relative to the lowest-energy structure 10a. This Al-encapsulated structure is listed in Fig. 1 as 10c. The Al atom falls into the center of Y_{10} frame, and this shape is similar to that of the Al-encapsulated ground states of $Ti_{10}Al$ [29], $Y_{10}Al$ [30], $Na_{10}Al$ [33], $Sc_{10}Al$ [34], $Pb_{10}Al$ [35], $Li_{10}Al$ [36], but with low symmetry C_1. Isomer 10c is predicted to be higher in energy than 10a by 1.353 eV (B3PW91), 1.751 eV (B3LYP), 1.571 eV (PBEPBE).

In a word, the ground state geometries of the Nb_nAl clusters can be obtained by replacing one of the Nb atoms of the Nb_{n+1} clusters or by adding one Al atom on the stable Nb_n clusters with small local distortion. Al atoms always occupy the surface of the clusters and structure transition is not found in the present calculation, this may be due to the much larger bond strength of Nb-Nb bond (2.973 eV) than that of Nb-Al bond (1.993 eV).

Binding energy

The stability of Nb_nAl clusters is investigated using three methods based on their average binding energy, calculated as

$$E_b(Nb_nAl) = [nE(Nb) + E(Al) - E(Nb_nAl)]/(n+1)$$

where E(Nb),E(Al) and E(Nb_nAl) represent the total energies of the most stable Nb, Al and Nb, Al clusters, respectively.

The average binding energy has been plotted in Fig. 2 as a function of the number of Nb atom present in the cluster. The calculations yield a monotonic increase with the size n. The increased binding energy along with the cluster size can be found in most clusters. The trend of three curves obtained by three functionals is consistent, and the only different is that the PBEPBE method gives a bit higher average binding energy than the B3PW91 and B3LYP methods. From the growth trend, the Nb, Al cluster can continue to gain energy during the growth process. The binding energy of pure Nb_n has been investigated in Ref 15. Comparing the curve of pure Nb_n with that of doped Nb_nAl cluster, it can be found that the average binding energies of the Nb_n and Nb_nAl clusters vary in a similar way. When Al atom is doped the Nb_n cluster, the average binding energy is decreased. The smaller binding energy of doped Nb_nAl cluster relative to the pure Nb_n cluster may associate the significantly larger Nb-Nb bond than Nb-Al bond.

Ionization potential

The vertical ionization potentials (VIPs) of Nb_n and Nb_nAl are determined in Table 2 and Fig. 3 by using the B3PW91 method. The VIP corresponds to the difference in energy between neutral and cationic clusters keeping the atomic positions unaltered. The calculated VIPs of Nb_n are in good agreement with the measured values, except Nb_5 having a little deviation between the calculated and experimental values. From Fig. 3, the VIPs decrease with the increasing size of clusters up to n=7, and then show a odd-even alternation phenomenon with cluster size 7≤n≤11. Several groups investigated the VIPs of Nb_n, CISD calculation [4] yielded the VIPs of 4.85, 4.33, and 4.31eV for Nb_2, Nb_3, and Nb_4, respectively. These values are substantially smaller than the measured values. Nhat and coworker [22]

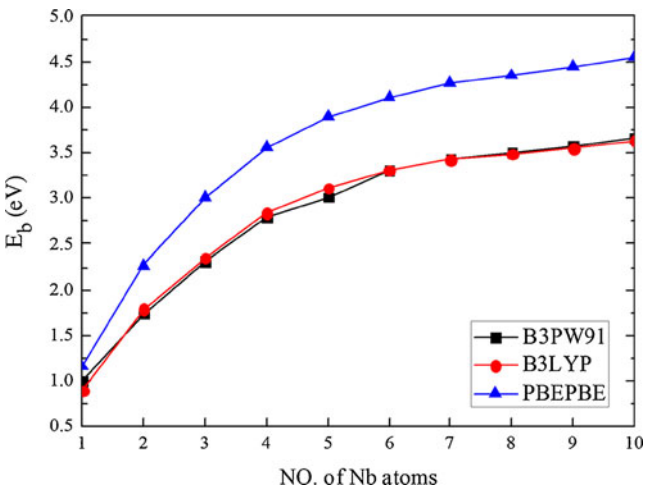

Fig. 2 The binding energy of Nb_nAl using B3PW91, B3LYP, and PBEPBE functionals

Table 2 The vertical ionization potentials (VIPs) of Nb_n and Nb_nAl by using the B3PW91 method

System	VIP		System	VIP
	Calc.	Expt.[a]		
Nb_2	6.344	6.2	NbAl	6.495
Nb_3	5.928	5.81	Nb_2Al	6.131
Nb_4	5.120	5.64	Nb_3A	6.036
Nb_5	5.120	5.45	Nb_4Al	5.341
Nb_6	5.258	5.38	Nb_5Al	5.677
Nb_7	5.187	5.35	Nb_6Al	5.177
Nb_8	5.413	5.53	Nb_7Al	5.013
Nb_9	5.142	5.20	Nb_8Al	5.148
Nb_{10}	5.473	5.48	Nb_9Al	4.980
Nb_{11}	4.563	4.74	$Nb_{10}Al$	5.301

[a] Ref [4]

calculated the VIPs of $Nb_n(2\leq n\leq 6)$ with different methods and the results agree with the experiments. The doped Nb_nAl clusters show different behavior compared with pure Nb_n, the trend of VIPs of Nb_nAl shows an odd-even alternation phenomenon. It is found that except for n=3 and 5, the values of VIP of Nb_nAl are smaller than corresponding pure Nb_n cluster. Comparison of the VIP between Nb_n and Nb_nAl clusters shows that the ionization potentials of Nb_n clusters decrease in presence of an Al atom.

Fragmentation behavior

The fragmentation behavior of a series of clusters bears significance in terms of understanding the abundance spectrum and the relative stability among smaller size clusters. Fragmentation energies of the Nb_nAl clusters were obtained

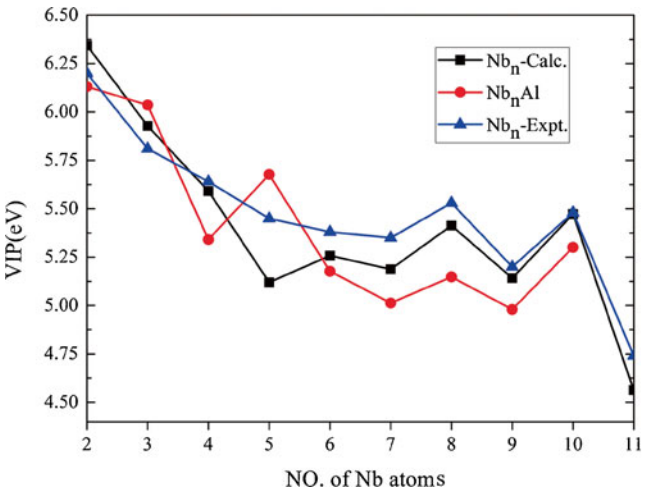

Fig. 3 The vertical ionization potentials (VIPs) of Nb_n and Nb_nAl by considering the B3PW91 functional

with respect to the reactions losing one Nb_i(i=1–10). The fragmentation energy is defined as:

$$E_F(Nb_nAl) = E(Nb_{n-i}Al) + E(Nb_i) - E(Nb_nAl).$$

A theoretical understanding of the fragmentation process is difficult and two factors can influence the preferred fragmentation path. First, the energy needed to dissociate a cluster into binary fragments. The second point concerns the barrier height for such a dissociation to occur. Table 3 gives all possible fragmentation pathways and their fragmentation energies for Nb_nAl cluster by considering the B3PW91 method and we have assumed that the fragmentation occurs along the lowest-energy pathways with no activation barrier.

It is clear from Table 3 that the lowest-energy channel is always via the Al dissociation from the Nb_nAl cluster, and this is similar to the dissociation pathway of Si_nAl where Al atom removal always produces the lowest-energy channel for Si_nAl clusters. Another competitive dissociation path is

Table 3 Fragmentation channels of the Nb_nAl clusters by considering the B3PW91 functional. The second columns indicate the fragmentation channel by $E_F(Nb_nAl) = E(Nb_{n-i}Al) + E(Nb_i) - E(Nb_nAl)$

System	Nb_i	E_F	System	Nb_i	E_F
Nb_2Al	Nb_1	3.205	Nb_8Al	Nb_1	4.079
	Nb_2	2.225		Nb_2	5.398
Nb_3Al	Nb_1	4.039		Nb_3	6.672
	Nb2	4.270		Nb_4	6.772
	Nb_3	2.940		Nb_5	7.607
Nb_4Al	Nb_1	4.739		Nb_6	7.326
	Nb_2	5.805		Nb_7	5.535
	Nb_3	5.686		Nb_8	2.622
	Nb_4	3.175	Nb_9Al	Nb_1	4.250
Nb_5Al	Nb_1	4.604		Nb_2	5.355
	Nb_2	6.370		Nb_3	6.324
	Nb_3	7.085		Nb_4	6.417
	Nb_4	5.786		Nb_5	7.117
	Nb_5	3.875		Nb_6	7.537
Nb_6Al	Nb_1	4.598		Nb_7	6.580
	Nb_2	6.228		Nb_8	4.878
	Nb_3	7.644		Nb_9	3.099
	Nb_4	7.178	$Nb_{10}Al$	Nb_1	4.497
	Nb_5	6.479		Nb_2	5.773
	Nb_6	4.153		Nb_3	6.528
Nb_7Al	Nb_1	4.293		Nb_4	6.316
	Nb_2	5.917		Nb_5	7.010
	Nb_3	7.197		Nb_6	7.294
	Nb_4	7.432		Nb_7	7.038
	Nb_5	7.567		Nb_8	6.170
	Nb_6	6.452		Nb_9	5.602
	Nb_7	3.450		Nb_{10}	2.175

achieved via the Nb-losing channel, which is the second lowest-energy channel for any cluster size. Figure 4 shows the plot for the dissociation energies of an Al or Nb atom from the Nb_nAl clusters. The dissociation energy of Al-losing channel rise up to n=6 and then follows a decreasing trend and finally shows an odd-even alternation behavior. In contrast to the behavior observed for Al-losing channel, the dissociation energy of Nb-losing channel shows continuous increase up to n=4 and then follows a decreasing trend and finally increases again at n=8. It can be found that the energy required to dissociate Nb atom is higher than Al atom for Nb_nAl clusters. The dissociation channel losing Al atom gives the large dissociation energy at n=6 and yields the small energy at n=8 and 10, the small energy of Al atom evaporation at n=8 and 10 is due to the fact that 8- and 10- atom Nb clusters have higher stability, leading to the dissociation path easily obtained. The channel losing Nb atom yields the largest dissociation energy at n=4. This indicates that Nb_4Al is energetically more stable than its neighbors, which may be attributed to the favored 18-electron configuration of Nb_4Al cluster. The smallest dissociation energy occurs at n=8, suggesting that Nb_8Al is less stable than others. Nb_6Al also has relatively large dissociation energy in all sizes of Nb_nAl clusters calculated here.

Charge transfer

Natural population analysis (NPA) results of Al atom in Nb_nAl clusters and the electronic population at a series of valent orbitals of Al and Nb atoms are determined in Tables 4 and 5, and the results are plotted in Figs. 5 and 6. From Fig. 5, charges always transfer from the doped Al atom to Nb atoms along with an odd-even phenomenon, which indicates that Al acts as electron donor in all Nb_nAl clusters. This is different from the results of Ti_nAl and Y_nAl clusters where the charge transfers from host atoms Ti and Y to doped atom Al, which may be caused by the smaller electronegativity of Ti (1.54) and Y (1.22) and almost the same values of Nb (1.6) compared to that of Al (1.61) atom. From Table 5, the positive charge of Al atoms in Nb_nAl clusters indicates that the 3s electrons of Al atom are transferred not only to its own 3p orbitals but also to the 4d or 5p orbital of Nb atoms. The 4s electrons of Nb are mainly transferred to the 4d and 5p orbital. From Fig. 6, for the Al atom the 3s orbital loses electrons about 0.2–0.5, and the 3p orbital gets electrons 0.05–0.36 with the exception of NbAl and $Nb_{10}Al$. The trend of 3p curve seems to have an opposite odd-even phenomenon to that of total charge transfer. For Nb atom, the ground state electronic configuration of the Nb atom is $4d^45s^1$. NPA results reveal that there are about 0.3 electrons transferred form 5s to 4d. There are about 0.06–0.37 electrons transferred to 5p orbital in which the electron numbers increase slowly along with the cluster size.

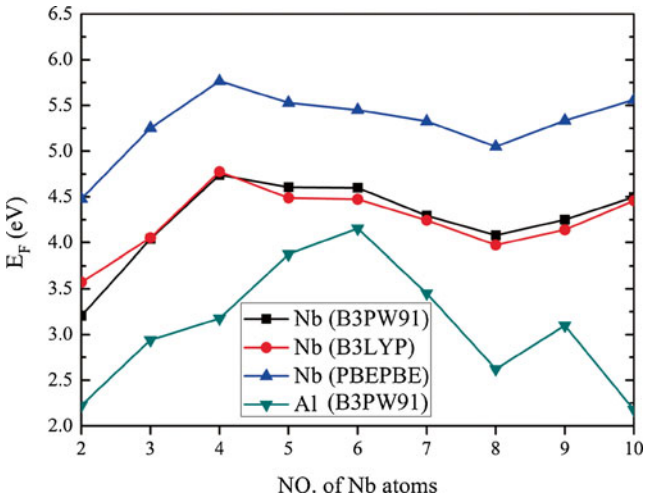

Fig. 4 The fragment energies of Al and Nb atoms from Nb_nAl clusters

Table 4 The charge of Al atom in the Nb_nAl clusters using B3PW91, B3LYP, and PBEPBE methods

System	B3PW91	B3LYP	PBEPBE
NbAl	0.217	0.224	0.225
Nb_2Al	0.186	0.194	0.234
Nb_3Al	0.235	0.250	0.283
Nb_4Al	0.423	0.423	0.421
Nb_5Al	0.340	0.344	0.355
Nb_6Al	0.482	0.482	0.495
Nb_7Al	0.441	0.445	0.463
Nb_8Al	0.575	0.566	0.546
Nb_9Al	0.574	0.562	0.583
$Nb_{10}Al$	0.654	0.591	0.604

Table 5 The natural population analysis of 3s and 3p orbitals for the Al atom and the average natural population analysis of 4d, 5s, and 5p orbitals for the Nb atom by considering B3PW91 functional. The results of degenerate structure 2b in parentheses

System	3s	3p	5s	4d	5p
NbAl	1.84	0.93	0.76	4.4	0.06
Nb_2Al	1.57(1.64)	1.23(1.14)	1.04(0.59)	3.92(4.41)	0.18(0.15)
Nb_3Al	1.55	1.2	0.687	4.223	0.203
Nb_4Al	1.51	1.05	0.64	4.23	0.27
Nb_5Al	1.38	1.26	0.578	4.228	0.308
Nb_6Al	1.24	1.26	0.55	4.28	0.317
Nb_7Al	1.18	1.36	0.514	4.32	0.289
Nb_8Al	1.25	1.16	0.505	4.268	0.356
Nb_9Al	1.25	1.17	0.482	4.28	0.366
$Nb_{10}Al$	1.36	0.97	0.468	4.332	0.334

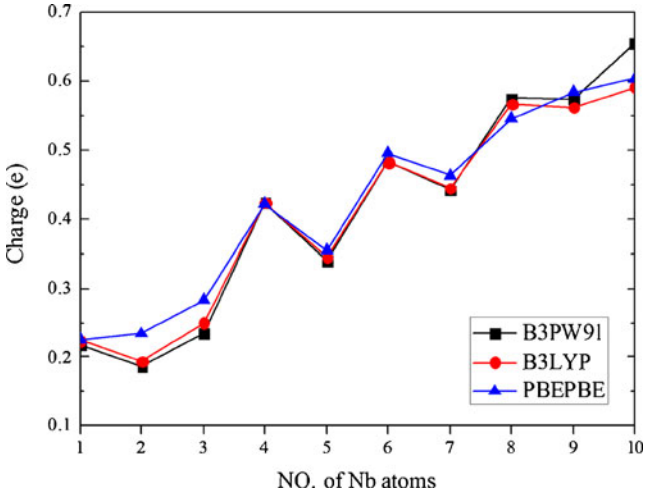

Fig. 5 Charge of Al atom in Nb_nAl clusters

Magnetic properties

The total magnetic moments of Nb_nAl ($1 \leq n \leq 10$) as well as the local magnetic moments of Zn and Nb atoms in Nb_nAl clusters are presented in Fig. 7 to investigate the size dependence. From Fig. 7a, the total magnetic moment is mainly located on the Nb atoms and Al atom only carries very small magnetic moment. The Nb_nAl clusters have total magnetic moments $1\mu_B$ for even n, in which the magnetism may come from the odd number of valence electrons. Whereas for odd n, the magnetic moments of Nb_5Al, Nb_7Al and Nb_9Al clusters are completely quenched.

To further illustrate the magnetic nature of the Nb_nAl clusters, we performed a detailed analysis of local magnetic moment of Nb atom in Nb_nAl clusters by NPA calculation. The charges of 4d, 5s, and 5p states for Nb atoms in Nb_nAl clusters are summarized in Fig. 7b. Figure 7b shows the

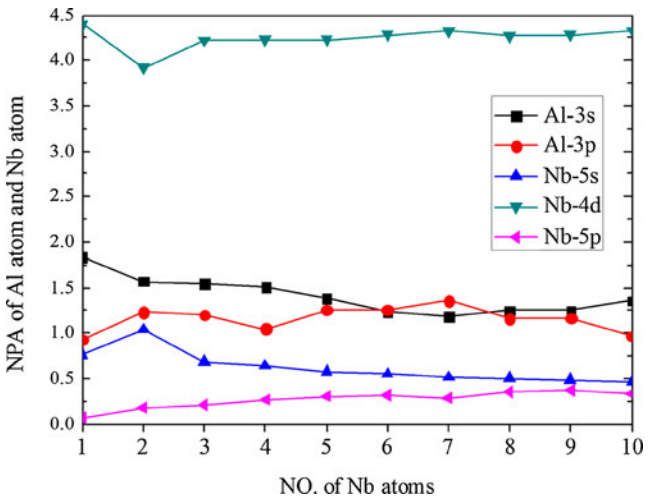

Fig. 6 The natural population analysis of 3s and 3p orbitals for the Al atom and the average natural population analysis of 4d, 5s, and 5p orbitals for the Nb atom by considering B3PW91 functional

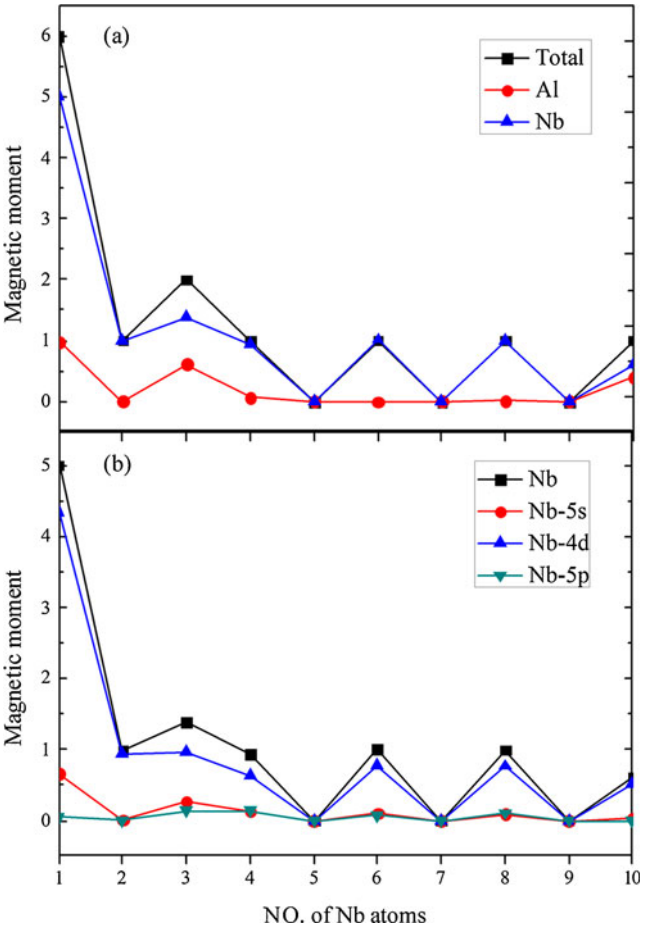

Fig. 7 **a** Total magnetic moments ($in\mu_B$) of Nb_nAl clusters and local magnetic moments of the Al and Nb atoms. **b** Magnetic moments ($in\mu_B$) of 4d, 5s, and 5p states for Nb atom in Nb_nAl clusters

magnetic moment of the Nb atoms is mainly from 4d state, following is the 5s and 5p states with small contribution to the magnetic moment of the Nb atoms.

Conclusions

We have identified the ground state geometries and studied the growth behavior, the electronic and magnetic properties of Nb_nAl species by means of three functionals. In contrast to the previously reported M_nAl cluster, where the shapes of ground state structures undergo a structural transition from the Al-capped frame to Al-encapsulated structure, in Nb_nAl clusters, Al atom always occupies the surface of clusters and structural transition does not take place until $n=10$ in the present calculation. The analysis of the fragmentation energy for Nb_nAl clusters shows that the energy required to dissociate an Al atom is lower than that of Nb atom. This may be attributed to the much larger Nb-Nb bond than Nb-Al bond. According to the NPA results, charges transfer from the doped Al atom to Nb atoms along with an odd-

even phenomenon, which indicates that Al acts as electron donor in all Nb_nAl clusters. This is different from the results of Ti_nAl andY_nAl clusters performed by Mulliken population analysis. The magnetism of the Nb_nAl clusters mostly stems from the contribution of 4d orbital of Nb atoms, and the contribution of magnetic moments of Al atom to the total magnetic moment is very small.

Acknowledgments This work was supported by the the National Natural science Foundation of China (Nos. 60838003 and 10774103).

References

1. Fielicke A, Ratsch C, Helden GV, Meijer G (2007) J Chem Phys 127:234306–234313
2. Pramann A, Nakajima A, Kaya K (2001) Chem Phys Lett 347:366–372
3. Knickelbein MB, Menezes WJC (1992) Phys Rev Lett 69:1046–1049
4. Knickelbein MB, Yang S (1990) J Chem Phys 93:5760–5767
5. Loh SK, Lian L, Armentrout PB (1989) J Am Chem Soc 111:3167–3176
6. Marcy TP, Leopold DG (2000) Int J Mass Spectrom 195–196:653–666
7. Kietzmann H, Morenzin J, Bechthold PS, Ganteför G, Eberhardt W, Yang DS, Hackett PA, Fournier R, Pang T, Chen CF (1996) Phys Rev Lett 77:4528–4531
8. Berg C, Schindler T, Niedner-Schatteburg G, Bondybey VE (1995) J Chem Phys 102:4870–4884
9. Bondybey VE, English JH (1981) J Chem Phys 74:6978–6979
10. Geusic ME, Morse MD, Smalley RE (1985) J Chem Phys 82:590–591
11. Morse MD, Geusic ME, Heath JR, Smalley RE (1985) J Chem Phys 83:2293–2304
12. Hamrick YM, Morse MD (1989) J Phys Chem 93:6494–6501
13. Radi PP, von Helden G, Hsu MT, Klemper PR, Bowers MT (1991) Int J Mass Spectrom Ion Process 109:49–73
14. Loh SK, Lian L, Armentrout PB (1989) J Chem Phys 91:6148–6163
15. Kumar V, Kawazoe Y (2002) Phys Rev B 65:125403–125413
16. Majumdar D, Balasubramanian K (2003) J Chem Phys 119:12866–12877
17. Majumdar D, Balasubramanian K (2001) J Chem Phys 115:885–898
18. Majumdar D, Balasubramanian K (2004) J Chem Phys 121:4014–4032
19. Goodwin L, Salahub DR (1993) Rhys Rev A 47:R774–R777
20. Fowler JE, Garcia A, Ugalde JM (1999) Phys Rev A 60:3058–3070
21. Zhai HJ, Wang B, Huang X, Wang LS (2009) J Phys Chem A 113:3866–3875
22. Nhat PV, Ngan VT, Nguyen MT (2010) J Phys Chem C 114:13210–13218
23. Grönbeck H, Rosén A (1996) Phys Rev B 54:1549–1552
24. Xie Y, He SG, Dong F, Bernstein ER (2008) J Chem Phys 128:044306–044314
25. Berces A, Hackett PA, Lian L, Mitchell SA, Rayner DM (1998) J Chem Phys 108:5476–5490
26. Holmgren L, Andersson M, Rosen A (1995) Surf Sci 331–333:231–236
27. Grönbeck H, Rosén A, Andreoni W (1998) Phys Rev A 58:4630–4636
28. Fournier R, Pang T, Chen CF (1998) Phys Rev A 57:3683–3691
29. Xiang J, Wei SH, Yan XH, You JQ, Mao YL (2004) J Chem Phys 120:4251–4257
30. Zhao GF, Zhang J, Jing Q, Luo YH, Wang YX (2007) J Chem Phys 127:234312–234318
31. Majumder C, Kulshreshtha SK (2004) Phys Rev B 69:115432–115439
32. Feng XJ, Luo YH (2007) J Phys Chem A 111:2420–2425
33. Dhavale A, Shah V, Kanhere DG (1998) Phys Rev A 57:4522–4527
34. Tian FY, Jing Q, Wang YX (2008) Phys Rev A 77:013202–013209
35. Chen DL, Tian WQ, Sun CC (2007) Phys Rev A 75:013201–013208
36. Cheng HP, Barnett RN, Landman U (1993) Phys Rev B 48:1820–1824
37. Frisch MJ, Trucks GW, Schlegel HB et al. (2004) Gaussian 03 Revision E.01. Gaussian, Inc, Wallingford, CT
38. Roy D, Corminboeuf C, Wannere CS, King RB, Schleyer PvR (2006) Inorg Chem 45:8902–8906
39. Bera PP, Sattelmeyer KW, Saunders M, Schaefer HF, Schleyer PvR (2006) J Phys Chem A 110:4287–4290
40. Saunders M (2004) J Comput Chem 25:621–626
41. Becke AD (1993) J Chem Phys 98:5648–5652
42. Perdew JP (1991) In: Ziesche P, Eschrig H (eds) Electronic structure of solids. Akademie, Berlin
43. Perdew JP, Chevary JA, Jackson SH, Jackson KA, Pederson MR, Singh DJ, Fiolhais C (1992) Phys Rev B 46:6671–6687
44. Perdew JP, Wang Y (1992) Phys Rev B 45:13244–13249
45. Lee C, Yang W, Parr RG (1988) Phys Rev B 37:785–789
46. Perdew P, Burke K, Ernzerhof M (1996) Phys Rev Lett 77:3865–3868
47. Wang HQ, Kuang XY, Li HF (2010) Phys Chem Chem Phys 12:5156–5165
48. Li HF, Kuang XY, Wang HQ (2011) Phys Lett A 375:2836–2844